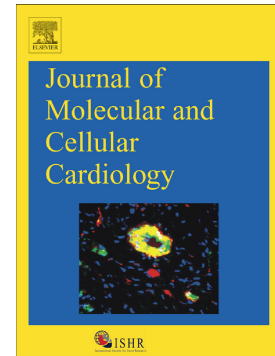


Journal Pre-proof

Cathelicidin aggravates myocardial ischemia/reperfusion injury via activating TLR4 signaling and P2X7R/NLRP3 inflammasome

Yan Wu, Yacheng Zhang, Jie Zhang, Tingting Zhai, Jingping Hu, Hairong Luo, Haiyan Zhou, Qinghai Zhang, Zhiguang Zhou, Feng Liu



PII: S0022-2828(20)30005-5

DOI: <https://doi.org/10.1016/j.yjmcc.2019.12.011>

Reference: YJMCC 9113

To appear in: *Journal of Molecular and Cellular Cardiology*

Received date: 18 August 2019

Revised date: 1 December 2019

Accepted date: 20 December 2019

Please cite this article as: Y. Wu, Y. Zhang, J. Zhang, et al., Cathelicidin aggravates myocardial ischemia/reperfusion injury via activating TLR4 signaling and P2X7R/NLRP3 inflammasome, *Journal of Molecular and Cellular Cardiology*(2020), <https://doi.org/10.1016/j.yjmcc.2019.12.011>

This is a PDF file of an article that has undergone enhancements after acceptance, such as the addition of a cover page and metadata, and formatting for readability, but it is not yet the definitive version of record. This version will undergo additional copyediting, typesetting and review before it is published in its final form, but we are providing this version to give early visibility of the article. Please note that, during the production process, errors may be discovered which could affect the content, and all legal disclaimers that apply to the journal pertain.

© 2020 Published by Elsevier.

Cathelicidin Aggravates Myocardial Ischemia/Reperfusion Injury via Activating TLR4 Signaling and P2X₇R/NLRP3 Inflammasome

Yan Wu,^{1,2} Yacheng Zhang,^{1,2} Jie Zhang,^{1,2} Tingting Zhai,^{1,2} Jingping Hu,^{1,2} Hairong Luo,^{1,2}
Haiyan Zhou,^{1,2} Qinghai Zhang,^{1,2} Zhiguang Zhou,^{1,2,*} and Feng Liu^{1,2,3,*}

¹Department of Metabolism and Endocrinology, Second Xiangya Hospital, Central South University, Changsha, Hunan 410011, China; ²National Clinical Research Center for Metabolic Diseases, Metabolic Syndrome Research Center, Second Xiangya Hospital, Central South University, Changsha, Hunan 410011, China; ³Department of Pharmacology, University of Texas at San Antonio, San Antonio, Texas, 78229, USA

***denotes equal contribution**

Corresponding Authors: Drs. Feng Liu (liuf@utmscsa.edu) and Zhiguang Zhou (zhouzhiguang@csu.edu.cn), Department of Metabolism and Endocrinology, Second Xiangya Hospital, Central South University, No.139 Middle Renmin Road, Changsha, Hunan 410011, China. Tel/Fax: +86 0731 85292148

Running Title: Cathelicidin and ischemia/reperfusion injury

Category: Original Article

Abstract

Aims: The antimicrobial peptide cathelicidin (*Camp*) has multifunctional immunomodulatory activities. However, its roles in inflammation-related myocardial ischemia/reperfusion (MI/R) injury remain unclear.

Methods and results: In this study, adult male C57BL/6 wild-type (WT) mice were subjected to MI/R injury by left anterior descending coronary artery ligation for 45 minutes followed by 3 or 24 hours of reperfusion. An abundant cardiac expression of cathelicidin was observed during ischemia and reperfusion, which was mainly derived from heart-infiltrating neutrophils. Knockout of *Camp* in mice reduced MI/R-induced myocardial inflammation, infarct size, and circulating cTnI levels (an indicator of heart damage). CRAMP (the mature form of murine cathelicidin) administration of WT mice immediately before MI/R exerted detrimental effects on the reperfused heart. CRAMP exacerbates MI/R injury via a TLR4 and P2X₇R/NLRP3 inflammasome-dependent mechanism, since MI/R-induced myocardial infarction was reserved by inhibition of TLR4, P2X₇R, or NLRP3 inflammasome in CRAMP-treated WT mice. Depletion of neutrophils before MI/R abrogated the amplification of infarct size in CRAMP-treated WT mice. Heart-infiltrating neutrophils were found to be one of major cellular sources of myocardial IL-1 β (the “first line” pro-inflammatory cytokine) at the early stage of MI/R. At this stage, CRAMP administration just before MI/R induced pro-IL-1 β protein expression in heart-infiltrating neutrophils, but not in non-neutrophils. *In vitro* experiments showed that LL-37 (the mature form of human cathelicidin) treatment promotes the processing and secretion of IL-1 β from human neutrophils via stimulating TLR4 signaling and P2X₇R/NLRP3 inflammasome.

Conclusions: Our findings reveal that, at the early stage of MI/R, neutrophil-derived cathelicidin plays an injurious role in the heart. Cathelicidin aggravates MI/R injury possibly by over-activating TLR4 signaling and P2X₇R/NLRP3 inflammasome in heart-infiltrating neutrophils, which leads to the excessive secretion of IL-1 β and subsequent inflammatory injury.

Keywords: Cathelicidin; neutrophils; TLR4; P2X₇R; NLRP3 inflammasome; ischemia/reperfusion

1. Introduction

Acute myocardial infarction (AMI), characterized by blockage of coronary blood flow, remains a leading cause of morbidity and mortality worldwide¹. Early reperfusion of occluded coronary artery is a prerequisite for salvaging ischemic myocardium, but rapid restoration of blood flow to the ischemic region paradoxically leads to additional tissue damage, which is referred to as myocardial ischemia/reperfusion (MI/R) injury and may account for up to 50% of final infarct size². Despite paramount clinical interests, no effective interventions are currently available to reduce MI/R injury in patients with AMI, demonstrating an incomplete understanding of the pathogenesis of MI/R injury.

The toll-like receptor 4 (TLR4) signaling pathway-induced inflammation has been considered to be a crucial link to MI/R injury. Blockage of TLR4 signaling via genetic depletion³ or pharmacological inhibitors⁴ attenuates I/R-induced myocardial inflammation and tissue injury. The P2X purinoreceptor 7 (P2X₇R) expression, the NACHT, LRR, and PYD domains-containing protein 3 (NLRP3) inflammasome levels, and IL-1 β release are observed to significantly increase in the infarcted heart at early stage⁵. P2X₇R aggravates cardiac dysfunction after myocardial infarction through inducing inflammatory responses via the NLRP3/IL-1 β pathway⁵. When exposed to MI/R injury, mice deficient in NLRP3⁶ or given with a NLRP3 inhibitor⁷ have a reduced myocardial IL-1 β level, smaller infarct size and better cardiac function than WT mice. Accordingly, targeting the early activation of P2X₇R/NLRP3 inflammasome to attenuate IL-1 β -mediated downstream inflammatory cascades has been proposed to protect the heart against MI/R injury.

The antimicrobial peptide cathelicidin is an evolutionarily conserved component of the innate immune system that plays a crucial role in protecting the host from a wide range of pathogens⁸. This peptide is found in neutrophils, epithelial cells, keratinocytes, lymphocytes, monocytes and mast cells and can be locally induced to a high level at the sites of inflammation and infection⁹. The cathelicidin gene *Camp* encodes a propeptide pro-CRAMP in mice and hCAP-15 in humans that is proteolytically cleaved to generate the mature bioactive peptide CRAMP¹⁰ or LL-37¹¹, in mice or in humans, respectively. CRAMP and LL-37 have many similarities in terms of structure, function and tissue distribution¹², suggesting that CRAMP is a functional homolog of LL-37 in mice. Besides its microbicidal activities, cathelicidin has been found to neutralize lipopolysaccharide (LPS)¹³ and activate a broad variety of receptors, such as the formyl-peptide receptor-like 1 (FPRL1), chemokine (C-X-C motif) receptor 2, and P2X₇R¹⁴, to mediate its multifunctional immunomodulatory activities¹⁵. In contrast to its established roles in the immune system, the roles of cathelicidin in cardiovascular diseases remain largely unknown. Several studies showed that cathelicidin mediates the development of atherosclerosis by activating platelet¹⁶, recruiting inflammatory monocytes¹⁷, and acting as a self-antigen¹⁸. However, a very recent study reported that the CRAMP peptide is reduced post-MI/R and protects against MI/R injury in mice¹⁹, raising a question on the *bona fide* role of cathelicidin in MI/R injury.

Here, we showed that neutrophil-derived cathelicidin is highly expressed in the ischemic and reperfused myocardium in mice and that this peptide contributes to MI/R injury via a TLR4 and P2X₇/NLRP3 inflammasome-dependent mechanism.

2. Methods

2.1 Animals

Male C57BL/6 wild-type (WT) mice were purchased from Hunan SJA Laboratory Animal (Changsha, China). *Camp* knockout (KO) mice (stock 017799) and *Ckmm-Cre* mice (stock 006475) were purchased from the Jackson Laboratory. *Tlr4* KO mice were a generous gift from Dr. Hongliang Li at Collaborative Innovation Center of Model Animal Wuhan University²⁰. *Tlr4*^{fl/fl} mice were kindly provided by Dr. Philipp E. Scherer at University of Texas Southwestern Medical Center²¹ and crossed with *Ckmm-Cre* mice²² to generate skeletal and cardiac muscle-specific *Tlr4* KO (*Tlr4*^{MKO}) mice. Littermates not carrying the *Ckmm-Cre* transgene (*Tlr4*^{fl/fl}) served as controls. Mouse genotypes were determined by PCR (Supplementary Figure 1A-E). All primer information can be found in Supplementary Table 1. All mice used in this study were on a C57BL/6 background. Age-matched WT littermates were used as experimental controls. Considering that male sex predisposes the animal to an earlier onset and worsened cardiac phenotype than that of females, all experiments were performed in 10-12-week-old male mice. All mice were housed in a pathogen-free and temperature-controlled environment with 12-hour light/dark cycles and received food and water *ad libitum*. All animal experiments conformed to the *Guide for the Care and Use of Laboratory Animals* published by the US National Institutes of Health (NIH Publication Eighth Edition, 2011) and were approved by the ethics committee of Central South University.

2.2 Reagents

CRAMP (GLLRKCGEKVGEKLLKIGQKIKNFFQKLVPQPEQ) and LL-37 (LLGDFFRKSKEKICVLEFKRIVQRIKDFLRNLVPRTES) were synthesized with 99% purity, as confirmed by mass spectroscopy by Kaijing Biotech (Shanghai, China). We purchased TAK242 from MedChem Express (cat. HY-11109), A-804598 (cat. S8752) and MCC950 (cat. S7809) from Selleck, 16673-34-0 from Aladdin (cat. C124772), clodronate liposomes (Clo-Lip) (cat. F70101C-A) and control liposomes (Con-Lip) (cat. F70101-A) from FormuMax Scientific, monoclonal anti-Ly6G neutralizing antibody (clone 1A8, cat. BP0075-1) and isotype (cat. BP0089) as a control from BioXCell, LPS (*Escherichia coli* 0111:B4) (cat. L2630) and ATP (cat. A2383) from Sigma-Aldrich.

2.3 Isolation of human peripheral blood neutrophils

This experiment was approved by the Ethics Committee of Central South University. Human peripheral blood neutrophils were isolated from anticoagulated whole blood of healthy adult male volunteers. Blood was carefully added to PolymorphprepTM (Axis-Shield, cat. AS1114683) in a 15 ml centrifuge tube. After centrifugation, the lower band of polymorphonuclear leukocytes (PMNs) were harvested. Erythrocyte contamination was

removed by ammonium chloride lysis buffer (0.83% (w/v) NH_4Cl , 10 mM HEPES-NaOH, pH7.4). Human neutrophils (1×10^6 cells/well) were suspended in RPMI1640 medium (Gibco) supplemented with 2% fetal bovine serum (FBS) (Gibco) and cultured in 24-well culture plates for stimulation experiments.

2.4 Murine MI/R model

Surgical procedures were performed as previously described²³. Briefly, mice were anesthetized by intraperitoneal (i.p.) injection of sodium pentobarbital (70 mg/kg), and ventilated with positive pressure on a TOPO™ Dual Mode Ventilator (Kent Scientific). Body temperature was maintained at 37°C with a heating pad (ATC-2000, WPI). The thoracotomy was performed and the left anterior descending coronary artery (LAD) was ligated with an 8-0 nylon monofilament suture with a section of PE-10 tubing placed over the LAD. The ligation was tightened to occlude the artery to induce ischemia. The occlusion was confirmed by observing the change of color (becoming pallor) of the anterior wall of the left ventricle (LV). After occlusion for 45 minutes, reperfusion was initiated by loosening the ligation by removing the tubing. Sham-operated mice underwent the same procedure without ligation.

2.5 Infarct size measurements

At 24 hours after reperfusion, the chest was re-opened and the LAD ligation was re-tied. 1% Evans blue (Sigma-Aldrich) was infused into the aorta and coronary arteries to visualize the area at risk for infarction (AAR). The LV was harvested and sliced into 4 transverse sections, which were incubated with 2% triphenyltetrazolium chloride (TTC) solution (Sigma-Aldrich) to visualize the unstained infarcted area (IA). Each section of the heart was imaged with a Motic SMZ168 stereoscopic zoom microscope (MOTIC) and a Moticom 2306 digital camera (MOTIC). Viable myocardium stained red, infarcted tissue appeared white, and remote non-ischemic myocardium was blue. IA, AAR, and the total LV area from each section were determined using Motic Images Plus 2.0 software. The AAR/LV ratio and the IA/AAR ratio were calculated to evaluate the homogeneity of surgery and the severity of myocardial infarction, respectively.

2.6 Quantitative real-time PCR

Total RNA was extracted from heart tissues, MACS sorted cells or cultured human neutrophils by using Trizol (Invitrogen) and quantified with a UV-Vis Q5000 spectrophotometer (Quawell). cDNA was synthesized using RevertAid First Strand cDNA Synthesis Kit (Thermo Fisher Scientific) according to the manufacturer's instructions and then amplified on an ABI 7900HT using FastStart Universal SYBR Green Master (Roche). Relative expression level of mRNAs was calculated by the comparative Ct (ΔCt) method using *Gapdh* as a housekeeping gene. The primers used are as follows: 5'-TCCACCACCCTGTTGCTGTA-3' and 5'-ACCACAGTCCATGCCATCAC-3' for mouse *Gapdh*; 5'-ACAGCCTCAAGATCATCAGC-3' and 5'-GGTCATGAGTCCTTCCACGAT-3' for human *Gapdh*; 5'-GGGGTGGTGAAGCAGTGTAT-3' and 5'-TGAACCGAAAGGGCTGTG-3' for *Camp*;

5'-GATAAGCTGGAGTCACAGAAGG-3' and 5'-TTGCCGAGTAGATCTCAAAGTG-3' for *Il-6*; 5'-GTCTGTGCTGACCCCAAGAAG-3' and 5'-TGGTTCCGATCCAGGTTTTTA-3' for *Ccl-2*; 5'-CGATGGGTTGTACCTTGTCTAC-3' and 5'-GCAGAGAGGAGGTTGACTTTC-3' for *Tnf- α* ; 5'-TGACGTCACCTGGAGTTGTACGG-3' and 5'-GGTTCATGTCATGGATGGTGC-3' for *Tgf- β* ; 5'-AGCTGAAGACCCTCAGGATGCG-3' and 5'-TCATTCATGGCCTTGTAGACACCTTG-3' for *Il-10*; 5'-GCCACTCTACAGCTGGA-3' and 5'-CAGTTATATCCTGGCCGCCT-3' for human *pro-IL-1 β* .

2.7 Western blotting

Murine heart tissues or MACS sorted cells were lysed in RIPA lysis buffer (Beyotime). Total protein concentration was measured using Pierce BCA Protein Assay Kit (Thermo Fisher Scientific). Equal amounts of protein lysates or equal volume of plasma (for the measurement of circulating pro-CRAMP) was separated by SDS-PAGE for pro-CRAMP, TLR4, pro-IL-1 β and GAPDH or 10-20% Tris-Tricine gels (Invitrogen, cat. EC6625A) for CRAMP. Separated proteins were then transferred onto PVDF membranes (MILL Life Sciences), blocked with 5% non-fat dry milk and incubated with appropriate primary antibodies against CRAMP (1:1000 dilution, Innovagen, cat. PA-CRPL-100), TLR4 (1:1000 dilution, Cell Signaling Technology, cat.14358), pro-IL-1 β (1:500 dilution, Cell Signaling Technology, cat. 63124), or GAPDH (1:1000 dilution, Cell Signaling Technology, cat. 2118) overnight at 4°C. Membranes were then washed with TBST and incubated with appropriately matched horseradish peroxidase (HRP)-conjugated secondary antibodies (1:5000 dilution, Promega) for 1 hour at room temperature (RT). Bands were visualized using Western lightning plus-ECL (PerkinElmer). Membranes were scanned with a Molecular Imager® ChemiDoc™ XRS+ Western Blot Detection System (BIO-RAD) for quantitative analysis using Image Lab™ software. The expression level of GAPDH or IgG served as an internal control for protein loading.

2.8 ELISA

Murine plasma cTnI (CUSABIO, cat. CSB-E08421m), IL-6 (4A biotech, cat. CME0006), CCL-2 (4A biotech, cat. CME0046) and TNF- α (eBioscience, cat. 88-7324-88) levels, as well as human IL-1 β (Invitrogen, cat. 88-7261-22) levels in cell culture supernatants were measured by commercially available ELISA kits according to the manufacturer's protocols.

2.9 Flow cytometry

For flow cytometric analysis of heart tissues, the chest was opened and the heart was perfused with cold PBS. Heart tissue was then removed, weighted, washed, minced and enzymatically digested with digestion buffer containing collagenase I (450 U/ml, Sigma-Aldrich, cat. C0130), collagenase XI (125 U/ml, Sigma-Aldrich, cat. C7657), Hyaluronidase (60 U/ml, Sigma-Aldrich, cat. H3506) and DNase-I (60 U/ml, Sigma-Aldrich, cat. D4527). The digested tissue was then filtered through a 40- μ m nylon mesh (Falcon) in FACS buffer (eBioscience).

After centrifugation and resuspension, absolute cell numbers were determined using a TC20™ automated cell counter (BIO-RAD). After blocking with anti-CD16/CD32 monoclonal antibody (clone 93, BioLegend, cat. 101320), the cells (1×10^6) were incubated using antibodies including APC/Cy7-CD45 (BioLegend, cat. 103116), PerCP/Cy5.5-CD11b (clone M1/70, BioLegend, cat. 101228), APC/Cy7-Ly6G (clone 1A8, BioLegend, cat. 127624), FITC-Ly6C (clone HK1.4, BioLegend, cat. 128005) and APC-F4/80 (clone BM8, BioLegend, cat. 123116) for surface staining. For intracellular labeling of CRAMP, the cells were fixed with Fixation Buffer (BioLegend, cat. 420801) and then resuspended in Intracellular Staining Perm Wash Buffer (BioLegend, cat. 421002). Resuspended cells were stained intracellularly with CRAMP (Innovagen, cat. PA-CRPL-100) or Isotype (Innovagen, cat. PA-0000-1000) followed by incubation with PE Donkey anti-rabbit IgG (clone Poly4064, BioLegend, cat. 406421). For flow cytometric analysis of blood, peripheral blood was collected into K₂EDTA-coated tubes (BD, cat. 365974). Erythrocytes were lysed by RBC lysis buffer (Invitrogen, cat. 00-4300-54), blocked with anti-CD16/CD32 monoclonal antibody (clone 93, BioLegend, cat. 101320), and then incubated with antibodies including APC/Cy7-CD45 (clone 30-F11, BioLegend, cat. 103116), PerCP/Cy5.5-CD11b (clone M1/70, BioLegend, cat. 101228), FITC-Ly6C (clone HK1.4, BioLegend, cat. 128005), APC-Ly6G (clone 1A8, BioLegend, cat. 127614). The samples were stored in FACS buffer at 4°C in the dark before analysis. Flow cytometry was carried out on a FACSCanto II flow cytometer (Becton Dickinson) and data were analyzed with FlowJo software (Tree Star).

2.10 MACS sorting

For MACS sorting of heart tissues, the heart was perfused with cold PBS, removed, minced and enzymatically digested. After enzymatic dissociation, the samples were passed through a 40- μ m cell strainer (Falcon), washed with autoMACS running buffer (Miltenyi Biotec), centrifuged and resuspended. The cells (1×10^6) were stained with PE-conjugated anti-Ly6G antibody (clone 1A8, BioLegend, cat. 127608) or PE-conjugated anti-F4/80 antibody (BM8, BioLegend, cat. 123110) washed with autoMACS running buffer and incubated with Anti-PE MicroBeads (Miltenyi Biotec). The cells were then loaded on a MACS® LS column (Miltenyi Biotec), which is placed in the magnetic field of a MACS Separator (Miltenyi Biotec), to collect magnetically labeled Ly6G⁺ or F4/80⁺ cells, which were adhered to columns, and flow-through (unlabeled Ly6G⁻ or F4/80⁻ cells). The flow-through was repeatedly subjected to the above operation using PE-conjugated anti-CD11b antibody (M1/70, BioLegend, cat. 101208) to finally collect the following cellular populations: Ly6G⁺, Ly6G⁻, CD11b⁺Ly6G⁻, CD11b⁻Ly6G⁻, F4/80⁺, CD11b⁺F4/80⁻, and CD11b⁻F4/80⁻. For all MACS sorting, two LVs were pooled for each group in each experiment. For MACS sorting of blood, peripheral blood was collected and erythrocytes were lysed by RBC lysis buffer (Invitrogen, cat. 00-4300-54). After incubation, the blood was centrifuged, and then the pellet was resuspended and a cell count was performed. The next staining and sorting for Ly6G⁺ cells in blood was the same as that of heart tissues. All collected cells were then subjected to Western blotting or real-time PCR. For Western blotting analysis, since the number of heart-infiltrating neutrophils is

small, we analyzed all the protein lysates obtained from the MACS sorting without protein quantification.

2.11 Echocardiography

Transthoracic echocardiography was performed in *Camp* KO mice and their WT littermates under normal conditions using a Vevo2100 imaging system (VisualSonics). Mice were anaesthetized with 3% isoflurane and oxygen at 2L/min on a mask. Two-dimensional parasternal long axis views of the LV were obtained for guided M-mode measurements of the LV internal diameter at the diastole end and the systole end, as well as the interventricular septal wall thickness and posterior wall thickness. All measurements were conducted at the level of the papillary muscles. The investigator was blinded to group assignment.

2.12 Statistical analysis

All data are expressed as mean \pm SEM. Two groups were compared using a two-tailed, unpaired Student's *t*-test. Comparisons between multiple groups were performed using one-way or two-way ANOVA followed by Bonferroni's *post hoc* test. GraphPad Prism 6.0 software (GraphPad Software, Inc., La Jolla, CA, USA) was used for statistical analysis. A value of $P < 0.05$ was considered to be statistically significant.

3. Results

3.1 Cathelicidin is induced in the murine myocardium by MI/R challenge

We examined the expression profile of cathelicidin in the myocardium using a mouse model of MI/R. *Camp* levels were low in the heart of mice subjected to a sham operation, whereas cardiac ischemia for 45 minutes led to a significant increase in *Camp* transcripts with the maximal expression observed in the ischemic area of the LV 3 hour post-reperfusion (**Figure 1A**). At the protein level, full-length cathelicidin expression was low in the sham-operated heart, but was significantly elevated upon ischemia, which was continually up-regulated 3 hours post-reperfusion (**Figure 1B**). The protein levels of the mature CRAMP peptide in the injured zone of the LV were markedly increased at both ischemia and 3 hours post-reperfusion (**Figure 1C**). No obvious alterations in plasma cathelicidin levels were detected at ischemia or 3 hours post-reperfusion (**Supplementary Figure 2**). These data suggest that MI/R-induced cathelicidin plays an important local role in the heart.

3.2 Cathelicidin is mainly derived from infiltrating neutrophils during MI/R

Next, we sought to determine the cellular origin of cathelicidin in the heart during ischemia and reperfusion. Flow cytometric analysis showed that, after cardiac ischemia, nearly all CRAMP-expressing cells simultaneously stained positive for the myeloid cell-specific marker CD11b and the neutrophil-specific marker Ly6G in both the injured (**Figure 2A**) and remote uninjured (**Supplementary Figure 3A**) myocardium, suggesting that ischemia-induced cathelicidin mainly originates from neutrophils in the heart. To confirm this, we utilized two different experimental approaches. First, we sorted CD11b⁺F4/80⁻ myeloid cells, F4/80⁺ macrophages, and CD11b⁻F4/80⁻ non-myeloid cells from the whole

hearts of WT or *Camp* KO mice by MACS sorting. Western blotting revealed that cathelicidin protein expression was detected only in CD11b⁺F4/80⁺ cells from sham-operated or ischemia-challenged WT but not *Camp* KO hearts (**Figure 2B**). By using the same method, cathelicidin was detected only in Ly6G⁺ neutrophils from sham-operated or ischemia-challenged WT hearts, but not in Ly6G⁻ non-neutrophils (**Figure 2C**). Next, we depleted neutrophils in WT mice by a single injection of anti-Ly6G neutralizing antibody or control IgG (**Supplementary Figure 4**). Neutrophil depletion before MI/R almost completely abolished ischemia-induced cathelicidin protein expression in both the injured (**Figure 2D**) and remote uninjured (**Supplementary Figure 3B**) zone of the LV. These data suggest that neutrophils are the major site where cathelicidin is released in the heart during ischemia.

Notably, ischemia significantly induced the mRNA and protein expression of cathelicidin in cardiac Ly6G⁺ cells (**Supplementary Figure 5A, B**). Given that ischemia for 45 minutes may not be sufficient to induce the *de novo* synthesis of cathelicidin, we speculated that the increase in cathelicidin levels at ischemia may be due to the infiltration of circulating neutrophils with highly expressed cathelicidin into the heart. Indeed, we found that, at steady state, circulating Ly6G⁺ cells had significantly higher cathelicidin mRNA and protein levels compared to heart-resident Ly6G⁺ cells (**Supplementary Figure 5C, D**). Upon ischemia, the number of neutrophils in the blood, remote non-ischemic zone and ischemic zone was markedly increased (**Supplementary Figure 5E-G**), suggesting a quick recruitment of circulating neutrophils into the injured myocardium through the uninjured region, leading to increased cardiac cathelicidin levels observed during ischemia.

Similarly, depletion of neutrophils before MI/R significantly attenuated reperfusion-induced cathelicidin protein expression in both the injured (**Figure 2E**) and remote uninjured (**Supplementary Figure 3C**) zone of the LV, suggesting that infiltrating neutrophils are a main cellular source of cathelicidin in the heart at early reperfusion.

3.3 MI/R-induced cathelicidin contributes to myocardial injury

To dissect the physiological function of MI/R-induced cathelicidin expression *in vivo*, we compared the extent of MI/R injury between *Camp* KO mice and WT littermates. Echocardiographic analysis revealed no cardiac functional deficits in *Camp* KO mice under basal conditions (**Supplementary Table 2**). Whereas AAR was similar between WT and *Camp* KO mice (**Figure 3A**), the IA/AAR ratio was greatly reduced in *Camp* KO mice compared with WT mice 24 hours post-reperfusion (**Figure 3A**). Meanwhile, plasma cardiac troponin I (cTnI) levels, an indicator of myocardial damage, were significantly declined in *Camp* KO mice compared to WT littermates (**Figure 3B**). Consistently, mice with CRAMP administration just before MI/R displayed larger infarct size (**Figure 3C**) and elevated circulating cTnI levels (**Figure 3D**). These data suggest that cathelicidin plays a detrimental role during MI/R.

3.4 *Camp* deficiency attenuates myocardial post-reperfusion inflammation

To test whether MI/R-induced cathelicidin influences myocardial inflammatory responses to reperfusion, we examined the expression of multiple pro-inflammatory genes in the heart 3 hours post-reperfusion. When compared to WT mice, *Camp* deficiency significantly decreased *Tnf- α* , *Il-6*, and *Ccl-2* transcript levels in the injured myocardium (**Figure 4A-C**), whereas no difference was found in the remote uninjured myocardium (**Supplementary Figure 6A-C**). The circulating levels of these pro-inflammatory cytokines were similar between *Camp* KO and WT mice (**Supplementary Figure 6D-F**). *Camp* depletion did not alter the expression of anti-inflammatory genes *Tgf- β* and *Il-10* in the whole heart 3 hours post-reperfusion (**Supplementary Figure 6G-J**). Flow cytometric analysis (**Figure 4D**) revealed that *Camp* deficiency significantly reduced the infiltration of CD11b⁺Ly6G⁺ neutrophils (**Figure 4E**) and CD11b⁺Ly6GLy6C^{hi} pro-inflammatory monocytes (**Figure 4F**) in the ischemic myocardium 24 hours post-reperfusion compared with WT mice. These data suggest that MI/R-induced cathelicidin stimulates a pro-inflammatory signaling at the sites of heart injury at early stage.

3.5 Cathelicidin exacerbates MI/R injury via activation of TLR4 signaling

Next, we attempted to clarify the molecular mechanism involved in the deleterious roles of cathelicidin in MI/R. TLR4 has been demonstrated to critically mediate myocardial inflammation and tissue injury in murine models of MI/R^{3,4}. Considering that MI/R-induced cathelicidin promotes local inflammation and heart damage in our experimental model, we asked whether its detrimental roles are mediated by directly or indirectly activating TLR4 signaling. Inhibition of TLR4 using TAK242, a selective inhibitor for TLR4, before MI/R completely abrogated the extension of myocardial infarction in CRAMP-treated WT mice 24 hours post-reperfusion (**Figure 5A**). Similar protection was also seen in *Tlr4* KO mice (**Figure 5B**). Moreover, TAK242 pretreatment fully reversed CRAMP-stimulated pro-inflammatory gene expression in the ischemic myocardium 3 hours post-reperfusion (**Figure 5C-E**). These data suggest that activation of TLR4 signaling is required for the action of cathelicidin during MI/R.

To further clarify in which types of cells TLR4 critically mediates the injurious roles of cathelicidin in MI/R, we generated skeletal and cardiac muscle-specific *Tlr4* KO (*Tlr4*^{MKO}) mice by crossing *Tlr4*^{fl/fl} mice to *Ckmm-Cre* mice (**Supplementary Figure 1A-E**). Ablation of TLR4 in cardiac myocytes exacerbated myocardial infarction in CRAMP-treated *Tlr4*^{MKO} mice 24 hours post-reperfusion (**Supplementary Figure 7A**). Similarly, cardiac macrophage depletion before MI/R by a single injection of clodronate liposomes (**Supplementary Figure 8**) led to a larger infarct size in CRAMP-treated WT mice (**Supplementary Figure 7B**). On the other hand, depletion of neutrophils before MI/R almost completely abrogated the amplification of infarct size in CRAMP-treated WT mice (**Supplementary Figure 7C**). These data suggest that neutrophils may be a major cellular target of cathelicidin during MI/R. Indeed, we found that, at ischemia, cardiac Ly6G⁺ neutrophils from the injured zone had a significant higher TLR4 protein expression compared to cardiac CD11b⁺Ly6G⁻ myeloid cells or CD11b⁻Ly6G⁻ non-myeloid cells (**Supplementary Figure 9**), supporting a pivotal

contribution of TLR4 signaling in neutrophils to the action of cathelicidin at the early stage of MI/R.

3.6 Cathelicidin aggravates MI/R injury in a P2X₇R/NLRP3 inflammasome-dependent manner

IL-1 β is a “first line” cytokine responsible for initiating the inflammatory cascade and plays a central role in promoting MI/R injury²⁴. Activated neutrophils are one of major sources of IL-1 β in inflammatory diseases. Based on the finding that the human cathelicidin LL-37 promotes the processing and release of IL-1 β from monocytes via the activation of P2X₇R²⁵, we asked whether cathelicidin contributes to MI/R injury via promoting IL-1 β secretion from neutrophils by stimulating TLR4 signaling (to induce pro-IL-1 β synthesis²⁶) and P2X₇R/NLRP3 inflammasome (to cleave pro-IL-1 β into its active form^{27,28}) (**Figure 6A**). Myocardial infarction was prevented by pretreating with A-804593 (a P2X₇R antagonist) (**Figure 6B**) or 16673-34-0 (a NLRP3 inflammasome inhibitor) (**Figure 6C**) in CRAMP-injected WT mice 24 hours post-reperfusion, indicating that cathelicidin exacerbates MI/R injury involving the activation of the P2X₇R/NLRP3 inflammasome pathway.

Using MACS sorting followed by Western blotting, we found that, at 3 hours after reperfusion, cardiac Ly6G⁺ neutrophils from the injured area had a pro-IL-1 β protein level comparable to that of cardiac Ly6G⁻ non-neutrophils (**Figure 6D**), suggesting that neutrophils are one of major cellular sources of myocardial IL-1 β at the early stage of MI/R. CRAMP administration of WT mice just before MI/R significantly induced the protein expression of pro-IL-1 β in cardiac Ly6G⁺ neutrophils, but not in Ly6G⁻ non-neutrophils, 3 hours post-reperfusion (**Figure 6D**), further supporting that neutrophils are a main cellular target of cathelicidin during MI/R. In agreement with this, *in vitro* experiments using neutrophils isolated from human peripheral blood showed that LL-37 greatly increased *pro-IL-1 β* mRNA levels, which was inhibited by TAK242 pretreatment (**Figure 6E**). Additionally, treating the cells with LL-37 or LPS+ATP, a positive control, rapidly induced the secretion of mature IL-1 β (**Figure 6F**), while pretreatment with TAK242, A-804598 or MCC950 (a NLRP3 inflammasome inhibitor) markedly suppressed this stimulatory effect of LL-37 or LPS+ATP on IL-1 β (**Figure 6F**). The data from *in vitro* experiments indicate that cathelicidin facilitates the processing and secretion of IL-1 β from neutrophils via stimulating TLR4 signaling and P2X₇R/NLRP3 inflammasome.

4. Discussion

Neutrophils, which are the first innate immune cell recruited to the injured myocardium following AMI³⁰, have long been considered as a key contributor to MI/R injury³¹. Clearance of neutrophils from the ischemic myocardium is critical for the resolution of inflammation and limitation of tissue injury³². Previous studies mainly focus on the mechanisms by which neutrophils are attracted to and activated in the I/R-challenged heart^{33,34}. However, how heart-infiltrating neutrophils contribute to MI/R injury remains largely elusive. In this study, we observed a significant increase in the number of circulating neutrophils and heart-infiltrating neutrophils as early as 45 minutes after ischemia, which is accompanied by

upregulation of cardiac cathelicidin expression at this time point, revealing a relatively prompt activation of the cardiac innate immune response³⁵. We showed that heart-infiltrating neutrophils are a major source of cathelicidin during ischemia and reperfusion, which leads to MI/R injury via activating the TLR4 and P2X₇R/NLRP3 inflammasome signaling pathways. In addition to the above mechanism, we further assume that neutrophil-secreted cathelicidin promotes local inflammation and heart injury partly by suppressing neutrophil apoptosis and/or promoting neutrophil recruitment, which results in the amplified inflammation and tissue damage via the uncontrolled release of neutrophil content at the ischemic sites, since LL-37 has been reported to prolong the life span of activated neutrophils via the activation of FPRL1 and P2X₇R³⁶ and chemoattract human peripheral blood neutrophils by interacting with FPRL1^{37,38}.

Although TLR4 has been demonstrated to play a critical role in the activation of inflammatory cells and cardiomyocyte injury following MI/R, the exact mechanisms responsible for its actions remain poorly understood. In this study, we showed that activation of TLR4 signaling is essential for the action of cathelicidin during MI/R, since blockade of TLR4 signaling by pharmacological inhibitor or genetic depletion almost fully abrogates the extension of infarct size in CRAMP-treated WT or *Tlr4* KO mice post-MI/R. Nevertheless, we also found that *Tlr4* deficiency in cardiac myocytes leads to a greater infarct size in CRAMP-treated *Tlr4*^{MKO} mice post-MI/R, demonstrating that TLR4 expressed on cardiomyocytes mediates a cardioprotective role in MI/R injury, which is in line with previous *in vitro* studies³⁹, and suggesting that cardiomyocytes are unlikely to be a main cellular target of cathelicidin during MI/R. Indeed, it has been reported that TLR4 signaling participates in LPS preconditioning induced cardiac protection in MI/R injury via iNOS- and soluble guanylate cyclase (sGC)-dependent mechanisms⁴⁰ and this protective role may be mediated by TLR4 expressed on cardiomyocyte. To the best of our knowledge, our study is the first to demonstrate the myocardial protection of cardiomyocyte TLR4 in MI/R injury by using cardiac muscle-specific *Tlr4* KO mice. However, the exact mechanisms by which cardiomyocyte TLR4 contributes to cardiac protection in MI/R injury remain unclear, which may be the same as that of TLR4 in LPS preconditioning and need to be further clarified. Based on these findings, we further speculate that TLR4 signaling in cardiomyocytes may protect the heart against CRAMP-induced myocardial injury in this study. However, we found that the protein levels of TLR4 in cardiomyocytes were much lower than that in heart-infiltrating neutrophils, and thus the cardiac protection mediated by cardiomyocyte TLR4 may be masked by the detrimental roles mediated by TLR4 in inflammatory cells in the ischemic heart. Also, it is impossible for macrophages to mediate the injurious roles of cathelicidin in MI/R, since macrophage depletion aggravates myocardial infarction in CRAMP-treated WT mice post-MI/R. In contrast, depletion of neutrophils almost fully abolished the deleterious effects of CRAMP on the MI/R-challenged myocardium. This made us to conclude that neutrophils might be a main cellular target of cathelicidin in the heart during MI/R, and thus direct or indirect activation of TLR4 signaling in neutrophils by cathelicidin might be a key mechanism by which TLR4 participates in MI/R injury. Notably, in this study, we did not rule out the possibility that TLR2 is involved in mediating the

activities of cathelicidin in our experimental model, since TLR2 has also been considered to mediate myocardial inflammation and tissue injury during MI/R⁴¹.

In addition to TLR4, we also found that P2X₇R, a known receptor for LL-37, is involved in mediating the activities of cathelicidin in MI/R injury. It is well-known that generation of active IL-1 β requires two separate stimuli: 1) a priming stimulus to promote the synthesis of pro-IL-1 β , such as LPS, which induces pro-IL-1 β synthesis through the activation of TLR4²⁶, and 2) a secretion stimulus to initiate the posttranslational processing and release of IL-1 β , such as extracellular ATP, which stimulates mature IL-1 β secretion through the engagement of P2X₇R^{27,28}. In this study, we showed that CRAMP aggravates MI/R injury in a TLR4 and P2X₇R/NLRP3 inflammasome-dependent manner, which made us to speculate that IL-1 β secretion stimulated by cathelicidin via activating TLR4 signaling and P2X₇R/NLRP3 inflammasome may be a key mechanism by which cathelicidin promotes myocardial inflammation and tissue injury. In support of this hypothesis, pro-IL-1 β was specifically induced in heart-infiltrating neutrophils by CRAMP administration during MI/R. Furthermore, our *in vitro* experiments showed that human cathelicidin LL-37 directly stimulated pro-IL-1 β mRNA expression and mature IL-1 β release from human neutrophils via a TLR4- and P2X₇R/NLRP3 inflammasome-dependent manner. In this study, although we did not exclude the possibility that CRAMP has a direct effect on cardiomyocyte death, the fact that inhibition of TLR4, P2X₇R or NLRP3 inflammasome almost fully abolished the deleterious effects of CRAMP administration on the I/R-challenged heart accompanied by attenuated inflammatory responses strongly supports the notion that the TLR4 and P2X₇R/NLRP3 inflammasome/IL-1 β signaling pathway-mediated inflammatory injury is a possible causative mechanism of MI/R injury in CRAMP-treated WT mice.

Interestingly, our finding that CRAMP protein levels were significantly increased in the ischemic area of I/R-challenged heart is contradictory to a very recent study, which showed reduced CRAMP protein levels in the infarct zone of I/R-challenged heart¹⁹. This discrepancy may be related to different time points. In our study, heart samples were collected at ischemia and 3 hours after reperfusion, whereas in the reported study, heart samples were analyzed 24 hours after reperfusion. In addition, different analytical methods may be one of the reasons for inconsistency. In our study, Western blotting was used to assess the mature CRAMP peptide levels in the myocardium, whereas Bei *et al.* utilized ELISA analysis to evaluate the protein levels of this peptide. Furthermore, myocardial full-length cathelicidin mRNA and protein levels were measured in our study, but not in the reported study. More importantly, we demonstrated that increased cathelicidin has a deleterious role in MI/R, which is in contrast to the findings of Bei *et al.* showing that the CRAMP peptide protects against MI/R injury¹⁹. It should be pointed out that the experimental designs in these two studies are different. First, in our study, the majority of experiments were carried out *in vivo* in a mouse model of MI/R, whereas in the reported study, most of the experiments were performed in a rat cell model of anoxia/reoxygenation. Second, the doses of CRAMP administration used in these two studies are different. In our study, the CRAMP peptide was administered i.p. just before MI/R at a single dose of 200 μ g per mouse as previously reported²⁹, whereas in the

reported study, mice were i.p. injected with the CRAMP peptide at 4 mg/kg/day for three consecutive days and then subjected to MI/R on the last day of CRAMP injection. Although these differences exist between the two studies, the exact reasons for the discrepancies remain unclear.

In the present study, one limitation is that we did not evaluate the clinical relevance of our findings. Several studies reported that systemic LL-37 levels are decreased in AMI patients compared to control patients^{19,42}. Active proteinase 3 (PR3), a well-known protease involved in hCAP-18 cleavage into LL-37⁴³, is partly released from circulating neutrophils and rapidly inactivated in sera by irreversible binding to SERPIN A1^{44,45}. Thus, little free PR3 exists in sera, and it is mainly present as a PR3-SERPIN A1 complex⁴⁴. Based on these findings, we speculate that the decreased serum LL-37 levels observed in AMI patients may be due to the increased inactivation of serum PR3, since a previous study has reported that serum levels of the PR3-SERPIN A1 complex are significantly increased in patients with AMI⁴⁶. Notably, it has been proposed that SERPIN A1, a serum-borne inhibitor for PR3, may not have rapid access to extravascular sites where PR3 could be released post-AMI⁴⁶. In agreement with this, local serum LL-37 levels in the culprit lesion are higher than that in the systemic circulation in patients with AMI⁴². These findings are consistent with our view that cathelicidin plays an important local role at the sites of inflammation and injury. Unfortunately, we did not evaluate the correlation of myocardial LL-37 levels with the severity of myocardial damage in patients with AMI, since it is difficult to obtain human heart samples. Additionally, we found that the protein levels of cathelicidin in the heart were significantly increased and peak 24 hours after MI induced by permanent coronary artery ligation, and then gradually drop to the basal levels 7 days after MI, which is parallel to the infiltration of neutrophils into the myocardium post-MI (data not shown). This result suggests that neutrophil-derived cathelicidin may also play a critical role in the cardiac remodeling post-MI, which needs to be clarified in the future studies.

In conclusion, our work uncovers a previously unrecognized mechanism underlying MI/R injury (**Supplementary Figure 10**). We showed that soon after cardiac ischemia occurs, circulating neutrophils are recruited to the sites of heart injury where full-length cathelicidin is released and cleaved into the mature CRAMP peptide, leading to a great increase in the local CRAMP protein levels. Cleaved cathelicidin over-activates TLR4 signaling and P2X₇R/NLRP3 inflammasome in infiltrating neutrophils, which may lead to the excessive secretion of IL-1 β from neutrophils and ultimately heart post-I/R damage.

Acknowledgments

We thank Dr. Hongliang Li at Collaborative Innovation Center of Model Animal Wuhan University, China for providing *Tlr4* KO mice, Dr. Philipp E. Scherer at University of Texas Southwestern Medical Center, USA for providing *Tlr4*^{fl/fl} mice, and Dr. Jean-Sébastien Silvestre at INSERM UMRS 970, France for expert technical assistance. This work was supported by the National Natural Science Foundation of China (No.81400352 and No.81200580) and the National Institutes of Health (R01 grant DK100697).

Conflict of interest: none declared.

References

1. Benjamin EJ, Blaha MJ, Chiuve SE, Cushman M, Das SR, Deo R, de Ferranti SD, Floyd J, Fornage M, Gillespie C, Isasi CR, Jiménez MC, Jordan LC, Judd SE, Lackland D, Lichtman JH, Lisabeth L, Liu S, Longenecker CT, Mackey RH, Matsushita K, Mozaffarian D, Mussolino ME, Nasir K, Neumar RW, Palaniappan L, Pandey DK, Thiagarajan RR, Reeves MJ, Ritchey M, Rodriguez CJ, Roth GA, Rosamond WD, Sasson C, Towfighi A, Tsao CW, Turner MB, Virani SS, Voeks JH, Willey JZ, Wilkins JT, Wu JH, Alger HM, Wong SS, Muntner P, American Heart Association Statistics Committee and Stroke Statistics Subcommittee. Heart Disease and Stroke Statistics-2017 Update: A Report From the American Heart Association. *Circulation* 2017;**135**:e146-e243.
2. Hausenloy DJ, Yellon DM. Myocardial ischemia-reperfusion injury: a neglected therapeutic target. *J Clin Invest* 2013;**123**:92-100.
3. Oyama J, Blais C Jr, Liu X, Pu M, Kobzik L, Kelly RA, Boarcier T. Reduced myocardial ischemia-reperfusion injury in toll-like receptor 4-deficient mice. *Circulation* 2004;**109**:784-789.
4. Shimamoto A, Chong AJ, Yada M, Shomura S, Takayama H, Fleisig AJ, Agnew ML, Hampton CR, Rothnie CL, Spring DJ, Pohlman TH, Shimpo H, Verrier ED. Inhibition of Toll-like receptor 4 with eritoran attenuates myocardial ischemia-reperfusion injury. *Circulation* 2006;**114**:I270-I274.
5. Yin J, Wang Y, Hu H, Li X, Xue M, Cheng W, Wang Y, Li X, Yang N, Shi Y. P2X7 receptor inhibition attenuated sympathetic nerve sprouting after myocardial infarction via the NLRP3/IL-1 β pathway. *Journal of Cellular and Molecular Medicine* 2017;**21**:2695-2710.
6. Kawaguchi M, Takahashi M, Hata T, Kashima Y, Usui F, Morimoto H, Izawa A, Takahashi Y, Masumoto J, Koyama J, Hongo M, Noda T, Nakayama J, Sagara J, Taniguchi S, Ikeda U. Inflammasome activation of cardiac fibroblasts is essential for myocardial ischemia/reperfusion injury. *Circulation* 2011;**123**:594-604.
7. Marchetti C, Chojnacki J, Toldo S, Mezzaroma E, Tranchida N, Rose SW, Federici M, Van Tassell BW, Zhang S, Abbate A. A novel pharmacologic inhibitor of the NLRP3 inflammasome limits myocardial injury after ischemia-reperfusion in the mouse. *J Cardiovasc Pharmacol* 2014;**63**:316-322.
8. Gallo RL, Kim KJ, Bernfield M, Kozak CA, Zanetti M, Merluzzi L, Gennaro R. Identification of CRAMP, a cathelin-related antimicrobial peptide expressed in the embryonic and adult mouse. *J Biol Chem* 1997;**272**:13088-13093.
9. Gudmundsson GH, Agerberth B. Neutrophil antibacterial peptides, multifunctional effector molecules in the mammalian immune system. *J Immunol Methods* 1999;**232**:45-54.
10. Pestonjamas VK, Huttner KH, Gallo RL. Processing site and gene structure for the murine antimicrobial peptide CRAMP. *Peptides* 2001;**22**:1643-1650.

11. Sørensen OE, Follin P, Johnsen AH, Calafat J, Tjabringa GS, Hiemstra PS, Borregaard N. Human cathelicidin, hCAP-18, is processed to the antimicrobial peptide LL-37 by extracellular cleavage with proteinase 3. *Blood* 2001;**97**:3951-3959.
12. Zaiou M, Gallo RL. Cathelicidins, essential gene-encoded mammalian antibiotics. *Journal of Molecular Medicine* 2002;**80**:549-561.
13. Golec M. Cathelicidin LL-37: LPS-neutralizing, pleiotropic peptide. *Annals of Agricultural & Environmental Medicine* 2007;**14**:1-4.
14. Vandamme D, Landuyt B, Luyten W, Schoofs L. A comprehensive summary of LL-37, the factotum human cathelicidin peptide. *Cell Immunol* 2012;**280**:22-35.
15. Scott MG, Davidson DJ, Gold MR, Bowdish D, Hancock RE. The human antimicrobial peptide LL-37 is a multifunctional modulator of innate immune responses. *J Immunol* 2002;**169**:3883-3891.
16. Pircher J, Czermak T, Ehrlich A, Eberle C, Gaitzsch E, Margat A, Grommes J, Saha P, Titova A, Ishikawaankerhold H. Cathelicidins prime platelets to mediate arterial thrombosis and tissue inflammation. *Nat Commun* 2018;**9**:1523.
17. Döring Y, Drechsler M, Wantha S, Kemmerich K, Dievens D, Vijayan S, Gallo RL, Weber C, Soehnlein O. Lack of neutrophil-derived CRAMP reduces atherosclerosis in mice. *Circ Res* 2012;**110**:1052-1056.
18. Mihailovic PM, Lio WM, Yano J, Zhao K, Zhou J, Chyu KY, Shah PK, Cercek B, Dimayuga PC. The cathelicidin protein CRAMP is a potential atherosclerosis self-antigen in ApoE(-/-) mice. *PLoS One* 2017;**12**:e187432.
19. Bei Y, Pan LL, Zhou Q, Zhao C, Xie Y, Wu C, Meng X, Gu H, Xu J, Zhou L, Sluijter J, Das S, Agerberth B, Sun J, Xiao J. Cathelicidin-related antimicrobial peptide protects against myocardial ischemia/reperfusion injury. *BMC Med* 2019;**17**:42.
20. Jiang DS, Zhang XF, Gao L, Zeng J, Zhou H, Liu Y, Zhang Y, Bian ZY, Zhu LH, Fan GC, Zhang XD, Li H. Signal regulatory protein- α protects against cardiac hypertrophy via the disruption of toll-like receptor 4 signaling. *Hypertension* 2014;**63**:96-104.
21. Jia L, Vianna CR, Fukuda M, Berglund ED, Liu C, Tao C, Sun K, Liu T, Harper MJ, Lee CE, Lee S, Scherer PE, Elmquist JK. Hepatocyte Toll-like receptor 4 regulates obesity-induced inflammation and insulin resistance. *Nat Commun* 2014;**5**:3878.
22. Brüning JC, Michael MD, Winnay JN, Hayashi T, Hörsch D, Accili D, Goodyear LJ, Kahn CR. A muscle-specific insulin receptor knockout exhibits features of the metabolic syndrome of NIDDM without altering glucose tolerance. *Mol Cell* 1998;**2**:559-569.
23. Wu Y, Lu X, Xiang FL, Lui EM, Feng Q. North American ginseng protects the heart from ischemia and reperfusion injury via upregulation of endothelial nitric oxide synthase. *Pharmacol Res* 2011;**64**:195-202.
24. Sager HB, Heidt T, Hulsmans M, Dutta P, Courties G, Sebas M, Wojtkiewicz GR, Tricot B, Iwamoto Y, Sun Y, Weissleder R, Libby P, Swirski FK, Nahrendorf M. Targeting Interleukin-1 β Reduces Leukocyte Production After Acute Myocardial Infarction. *Circulation* 2015;**132**:1880-1890.

25. Elssner A, Duncan M, Gavrilin M, Wewers MD. A novel P2X7 receptor activator, the human cathelicidin-derived peptide LL37, induces IL-1 beta processing and release. *J Immunol* 2004;**172**:4987-4994.
26. Zheng W, Zheng X, Liu S, Ouyang H, Levitt RC, Candiotti KA, Hao S. TNF α and IL-1 β are mediated by both TLR4 and Nod1 pathways in the cultured HAPI cells stimulated by LPS. *Biochem Biophys Res Commun* 2012;**420**:762-767.
27. Mutini C, Falzoni S, Ferrari D, Chiozzi P, Morelli A, Baricordi OR, Collo G, Ricciardi-Castagnoli P, Di Virgilio F. Mouse dendritic cells express the P2X7 purinergic receptor: characterization and possible participation in antigen presentation. *J Immunol* 1999;**163**:1958-1965.
28. Sandanger Ø, Ranheim T, Vinge LE, Bliksøen M, Alfsnes K, Finsen AV, Dahl CP, Askevold ET, Florholmen G, Christensen G, Fitzgerald KA, Lien E, Valen G, Espevik T, Aukrust P, Yndestad A. The NLRP3 inflammasome is up-regulated in cardiac fibroblasts and mediates myocardial ischaemia-reperfusion injury. *Cardiovasc Res* 2013;**99**:164-174.
29. Diana J, Simoni Y, Furio L, Beaudoin L, Agerberth B, Barrat F, Lehuen A. Crosstalk between neutrophils, B-1a cells and plasmacytoid dendritic cells initiates autoimmune diabetes. *Nat Med* 2013;**19**:65-73.
30. Prabhu SD, Frangogiannis NG. The Biological Basis for Cardiac Repair After Myocardial Infarction: From Inflammation to Fibrosis. *Circ Res* 2016;**119**:91-112.
31. Vinten-johansen J. Involvement of neutrophils in the pathogenesis of lethal myocardial reperfusion injury. *Cardiovasc Res* 2004;**61**:481-497.
32. Romson JL, Hook BG, Kunkel SL, Abrams GD, Schork MA, Lucchesi BR. Reduction of the extent of ischemic myocardial injury by neutrophil depletion in the dog. *Circulation* 1983;**67**:1016-1023.
33. Fan Q, Tao R, Zhang H, Xi H, Lu L, Wang T, Su M, Hu J, Zhang Q, Chen Q, Iwakura Y, Shen W, Zhang R, Yan X. Dectin-1 Contributes to Myocardial Ischemia/Reperfusion Injury by Regulating Macrophage Polarization and Neutrophil Infiltration. *Circulation* 2019;**139**:663-678.
34. Del Fresno C, Saz-Leal P, Enamorado M, Wculek SK, Martínez-Cano S, Blanco-Menéndez M, Schulz O, Gallizioli M, Miró-Mur F, Cano E, Planas A, Sancho D. DNCR-1 in dendritic cells limits tissue damage by dampening neutrophil recruitment. *Science* 2018;**362**:351-356.
35. Vilahur G, Hernández-Vera R, Molins B, Casaní L, Duran X, Padró T, Badimon L. Short-term myocardial ischemia induces cardiac modified C-reactive protein expression and proinflammatory gene (cyclo-oxygenase-2, monocyte chemoattractant protein-1, and tissue factor) upregulation in peripheral blood mononuclear cells. *J Thromb Haemost* 2009;**7**:485-493.
36. Nagaoka I, Tamura H, Hirata M. An antimicrobial cathelicidin peptide, human CAP18/LL-37, suppresses neutrophil apoptosis via the activation of formyl-peptide receptor-like 1 and P2X7. *J Immunol* 2006;**176**:3044-3052.

37. Tjabringa GS, Ninaber DK, Drijfhout JW, Rabe KF, Hiemstra PS. Human cathelicidin LL-37 is a chemoattractant for eosinophils and neutrophils that acts via formyl-peptide receptors. *Int Arch Allergy Immunol* 2006;**140**:103-112.
38. De Yang, Chen Q, Schmidt AP, Anderson GM, Wang JM, Wooters J, Oppenheim JJ, Chertov O. LL-37, the neutrophil granule- and epithelial cell-derived cathelicidin, utilizes formyl peptide receptor-like 1 (FPRL1) as a receptor to chemoattract human peripheral blood neutrophils, monocytes, and T cells. *J Exp Med* 2000;**192**:1069-1074.
39. Zhu X, Zhao H, Graveline A, Es, Schmidt U, Bloch K, Rosenzweig A, Chao W. MyD88 and NOS2 are essential for toll-like receptor 4-mediated survival effect in cardiomyocytes. *Am J Physiol Heart Circ Physiol* 2006;**291**:1900-1909.
40. Wang E, Feng Y, Zhang M, Zou L, Li Y, Buys ES, Huang P, Brouckaert P, Chao W. Toll-like receptor 4 signaling confers cardiac protection against ischemic injury via inducible nitric oxide synthase- and soluble guanylate cyclase-dependent mechanisms. *Anesthesiology* 2011;**114**:601-613.
41. Arslan F, Smeets MB, O'Neill LAJ, Keogh B, Mcguirk P, Timmers L, Tersteeg C, Hoefler IE, Doevendans PA, Pasterkamp G. Myocardial Ischemia/Reperfusion Injury Is Mediated by Leukocytic Toll-Like Receptor-2 and Reduced by Systemic Administration of a Novel Anti-Toll-Like Receptor-2 Antibody. *Circulation* 2010;**121**:80-90.
42. Zhao H, Yan H, Yamashita S, Li W, Liu C, Chen Y, Zhou P, Chi Y, Wang S, Zhao B, Song L. Acute ST-segment elevation myocardial infarction is associated with decreased human antimicrobial peptide LL-37 and increased human neutrophil peptide-1 to 3 in plasma. *J Atheroscler Thromb* 2012;**19**:357-368.
43. Sørensen OE, Follin P, Johnsen AH, Calafat J, Tjabringa GS, Hiemstra PS, Borregaard N. Human cathelicidin, hCAP-18, is processed to the antimicrobial peptide LL-37 by extracellular cleavage with proteinase 3. *Blood* 2001;**97**:3951-3959.
44. Bo B, Petersen J, Permin H, Wiik A, Wieslander J. Measurements of proteinase 3 and its complexes with α 1-antitrypsin inhibitor and Anti-Neutrophil Cytoplasm Antibodies (ANCA) in plasma. *Immunol Methods* 1994;**175**:215-225.
45. Durantou J, Bith G. Inhibition of proteinase 3 by [alpha]1-antitrypsin in vitro predicts very fast inhibition in vivo. *Am J Respir Cell Mol Biol* 2003;**29**:57-61.
46. Ng LL, Khan SQ, Narayan H, Quinn P, Squire IB, Davies JE. Proteinase 3 and prognosis of patients with acute myocardial infarction. *Clin Sci (Lond)* 2011;**120**:231-238.

Figure legends

Figure 1 The expression profile of cathelicidin in the I/R-challenged heart. (A) Cardiac *Camp* mRNA levels were evaluated by real-time PCR. The sham-operated heart was used as a control, and *Gapdh* as a housekeeping gene (n=3 mice per group). (B) Representative immunoblots of pro-CRAMP in sham-operated or I/R-challenged hearts (top) and semiquantification of band intensity (bottom). GAPDH was used as a loading control (n=4 mice per group). (C) Immunoblots showing pro-CRAMP, CRAMP and GAPDH abundance in the hearts from WT mice subjected to sham operation or I/R challenge (n=3 mice per group). Data are shown as mean \pm SEM. ** $P < 0.01$ and *** $P < 0.001$. NAAR, the non-area at risk for infarction; AAR, the area at risk for infarction.

Figure 2 Cellular sources of cathelicidin in the injured myocardium during ischemia and reperfusion. (A) WT mice were exposed to 45 minutes of ischemia, and then the injured myocardium was collected and subjected to flow cytometry for CRAMP, CD11b and Ly6G staining (representative of 3 independent experiments). (B) Immunoblots showing pro-CRAMP and GAPDH abundance in CD11b⁺F4/80⁻ myeloid cells, F4/80⁺ macrophages and CD11b⁻F4/80⁻ non-myeloid cells isolated from the whole hearts of WT or *Camp* KO mice subjected to sham operation or 45 minutes of ischemia by MACS sorting (n=3 independent experiments). (C) Immunoblots depicting pro-CRAMP and GAPDH expression in isolated Ly6G⁺ neutrophils and Ly6G⁻ non-neutrophils from the whole hearts of sham-operated or ischemia-challenged WT mice by MACS sorting (n=3 independent experiments). (D) WT mice were treated with monoclonal anti-Ly6G neutralizing antibody (100 μ g/mouse, i.p.) or isotype as a control. After 24 hours, the mice were subjected to 45 minutes of ischemia, and then the injured myocardium was collected and exposed to Western blotting. Representative

images of immunoblotting for pro-CRAMP (top) and semiquantification of band intensities (bottom) (n=3 mice per group). (E) After neutrophil depletion, pro-CRAMP protein expression was measured in the injured zone of the LV in WT mice subjected to 45 minutes of ischemia followed by 3 hours of reperfusion. Representative images of immunoblotting for pro-CRAMP (left) and semiquantification of band intensities (right) (n=3 mice per group). Data are shown as mean \pm SEM. * P < 0.05, ** P < 0.01 and *** P < 0.001. AAR, the area at risk for infarction.

Figure 3 Effects of cathelicidin deficiency or administration on MI/R injury. (A) Gross appearance of myocardial sections of the LV after Evans blue and TTC staining (top) (the infarct area is depicted with yellow line. scale bar, 1mm), and quantitative analysis for the area at risk for infarction (lower left) and the infarct area (lower right) in WT (n=12) and *Camp* KO (n=20) mice after 45 minutes of ischemia followed by 24 hours of reperfusion. (B) Plasma cTnI levels were analyzed in WT and *Camp* KO mice by ELISA 24 hours post-reperfusion (n=5 mice per group). (C,D) Effects of CRAMP (200 μ g/mouse, i.p.) injection just before MI/R on infarct size (n=8 mice per group. scale bar, 1mm) (C) and circulating cTnI levels (n=6 mice per group) (D) in WT mice 24 hours post-reperfusion. Data are shown as mean \pm SEM. ** P < 0.01 and *** P < 0.001. N.S., no significance; LV, the left ventricle; AAR, the area at risk for infarction; IA, the infarct area; I/R, ischemia/reperfusion.

Figure 4 Myocardial post-reperfusion inflammation is attenuated in *Camp* KO mice. (A-C) Real-time PCR analysis of *Tnf- α* (A) *Il-6* (B), and *Ccl-2* (C) in the injured area of the LV in WT and *Camp* KO mice subjected to 45 minutes of ischemia followed by 3 hours of reperfusion (n=6-8 mice per group). (D-F) Gating strategy of flow cytometry (D) and effects of *Camp* deficiency on the number of neutrophils (CD11b⁺Ly6G⁺) (E) and pro-inflammatory monocytes (CD11b⁺Ly6GLy6C⁺) (F) in the injured myocardium 24 hour post-reperfusion (n=6 mice per group). Data are shown as mean \pm SEM. * P < 0.05. AAR, the area at risk for infarction; I/R, ischemia/reperfusion.

Figure 5 Activation of TLR4 signaling is required for the action of CRAMP during MI/R. (A) WT mice were pretreated with TAK242 (0.5 mg/kg, i.p.) for 30 minutes followed by vehicle or CRAMP (200 μ g/mouse, i.p.) injection just before MI/R. Quantitative analysis of infarct size was performed 24 hour post-reperfusion (n=7-12 mice per group. scale bar, 1mm). (B) *Tlr4* KO mice and their WT littermates were injected with vehicle or CRAMP (200 μ g/mouse, i.p.) just before MI/R. Effects of *Tlr4* deficiency on infarct size were assessed 24 hours post-reperfusion (n=8-13 mice per group. scale bar, 1mm). (C-E) WT mice were pretreated with TAK242 (0.5 mg/kg, i.p.) for 30 minutes followed by vehicle or CRAMP (200 μ g/mouse, i.p.) administration immediately before MI/R. Quantification of *Tnf- α* (C), *Il-6* (D), and *Ccl-2* (E) gene expression in the injured region of the LV in WT mice 3 hours post-reperfusion (n=6 mice per group). Data are shown as mean \pm SEM. * P < 0.05, ** P < 0.01 and *** P < 0.001. N.S., no significance; LV, the left ventricle; AAR, the area at risk for infarction; IA, the infarct area; I/R, ischemia/reperfusion.

Figure 6 Activation of P2X₇R/NLRP3 inflammasome is essential for the activity of CRAMP during MI/R. (A) Proposed model for cathelicidin-activated inflammatory injury. (B,C) WT mice were pretreated with A-804598 (10 mg/kg, i.p.) for 1 hour (B) or 16673-34-0 (100 mg/kg, i.p.) for 30 minutes (C), followed by vehicle or CRAMP (200 µg/mouse, i.p.) injection just before MI/R. Quantitative analysis of infarct size was performed 24 hour post-reperfusion (n=8-10 mice per group. scale bar, 1mm). (D) WT mice were injected with vehicle or CRAMP (200 µg/mouse, i.p.) and then challenged to ischemia for 45 minutes followed by reperfusion for 3 hours. Ly6G⁺ and Ly6G⁻ cells were isolated from the injured myocardium by MACS sorting, and then analyzed for pro-IL-1β protein expression by Western blotting (n=3-4 mice per group). (E) Human peripheral blood neutrophils were isolated, pretreated with TAK242 (10 µM) for 30 minutes, and then stimulated with LL-37 (100 µg/ml) for 3 hours. Real-time PCR analysis of *pro-Il-1β* in the cells was carried out (n=3 independent experiments). (F) Human peripheral blood neutrophils were pretreated with TAK242 (10 µM) for 30 minutes and then primed with LL-37 (100 µg/ml) or LPS (20 ng/ml) for 3 hours. After which, the cells were incubated with ATP (5 mM) and A-804598 (10 µM) for 45 minutes with the pretreatment of MCC950 (1 µM) for 1 hour. The cell culture supernatants were collected for the measurement of IL-1β by ELISA (n=3 independent experiments). Data are shown as mean ± SEM. * *P* < 0.05, ** *P* < 0.01 and *** *P* < 0.001. N.S., no significance; LV, the left ventricle; AAR, the area at risk for infarction; IA, the infarct area; I/R, ischemia/reperfusion.

Supplementary data

Figure 1 Generation of mice lacking *Tlr4* in skeletal and cardiac muscle. (A) Targeting strategy for the conditional disruption of the *Tlr4* gene. (B) PCR analysis of tail-genomic DNA of mice bearing wild-type (wt) and/or floxed allele. PCR products of wt, floxed allele, and Cre are 260 bp, 343 bp, and 200 bp, respectively. (C) Schematic showing generation of *Tlr4*^{MKO} mice. *Tlr4*^{fl/fl} mice were mated to *Ckmm-Cre* mice to generate heterozygous mice (*Tlr4*^{fl/+}; *Ckmm-Cre*⁺), which crossed to *Tlr4*^{fl/fl} mice to obtain *Tlr4*^{MKO} (*Tlr4*^{fl/fl}; *Ckmm-Cre*⁺) mice. (D) PCR analysis of genomic DNA isolated from the indicated tissues of *Tlr4*^{MKO} mice. (E) Tissue expression of *Tlr4* in *Tlr4*^{MKO} and their *Tlr4*^{fl/fl} littermates (n=5 mice per group). Data are shown as mean ± SEM. ** *P* < 0.01. fl/fl, *Tlr4*^{fl/fl}; MKO, *Tlr4*^{MKO}.

Figure 2 Plasma cathelicidin concentrations during MI/R. WT mice were subjected to ischemia for 45 minutes followed by reperfusion for 3 hours. Plasma was collected to examine pro-CRAMP levels by Western blotting (n=3-4 mice per group). Plasma collected from sham-operated mice was used as a control, and IgG as a loading control. Data are shown as mean ± SEM. N.S., no significance.

Figure 3 Cellular sources of cathelicidin in the uninjured myocardium during ischemia and reperfusion. (A) WT mice were subjected ischemia for 45 minutes, and then the uninjured myocardium was collected for flow cytometry for CRAMP, CD11b, and Ly6G staining. Isotype was used as a negative control (representative of 3 independent experiments). (B,C) In WT mice, neutrophils were depleted by a single injection of

monoclonal anti-Ly6G neutralizing antibody (100 µg/mouse, i.p.) or isotype as a control. After 24 hours, the mice were subjected to ischemia for 45 minutes (B) followed by reperfusion for 3 hours (C), and then the uninjured myocardium was collected and analyzed for pro-CRAMP protein levels by Western blotting (n=3 mice per group). Data are shown as mean ± SEM. ** $P < 0.01$ and *** $P < 0.001$. NAAR, the non-area at risk for infarction.

Figure 4 Depletion of neutrophils in blood in mice. WT mice were injected with an anti-Ly6G neutralizing antibody (100 µg/mouse, i.p.) or isotype as a control to deplete neutrophils in blood. Flow cytometry was carried out to confirm the depletion of neutrophils in blood 24 hours after injection (n=3-4 mice per group). Data are shown as mean ± SEM. *** $P < 0.001$.

Figure 5 Ischemia-induced cardiac cathelicidin originates from heart-infiltrating neutrophils. (A,B) WT mice were subjected to sham-operation or ischemia for 45 minutes, and then Ly6G⁺ cells from the whole heart were isolated by MACS sorting. Quantitative analysis of *Camp* (A) and pro-CRAMP (B) levels was performed by real-time PCR and Western blotting, respectively (n=4 independent experiments). (C,D) Ly6G⁺ cells were sorted from blood and hearts of WT mice by MACS sorting under basal conditions, followed by real-time PCR analysis of *Camp* (C) or Western blotting analysis of pro-CRAMP (D) (n=4 independent experiments). (E-G) WT mice were subjected to 45 minutes of ischemia, and then blood (E), the uninjured (F) and injured (G) myocardium were collected to quantify neutrophils by flow cytometry. Blood and hearts from sham-operated mice were used as a control (n=5 mice per group). Data are shown as mean ± SEM. * $P < 0.05$ and *** $P < 0.001$. AAR, the area at risk for infarction; NAAR, the non-area at risk for infarction.

Figure 6 Effects of cathelicidin deficiency on pro-inflammatory cytokines in the uninjured myocardium and plasma, as well as anti-inflammatory cytokines in the heart post-MI/R. (A-C) WT and *Camp* KO mice were challenged to 45 minutes of ischemia followed by 3 hours of reperfusion. The mRNA levels of *Tnf-α* (A), *Il-6* (B), and *Ccl-2* (C) in the non-ischemic area of the LV were measured by real-time PCR (n=7-8 mice per group). (D-F) Plasma TNF-α (D), IL-6 (E), and CCL-2 (F) levels were measured by ELISA in WT and *Camp* KO mice 3 hours post-reperfusion (n=5-8 mice per group). (G,H) *Tgf-β* (G) and *Il-10* (H) mRNA levels were evaluated by real-time PCR in the ischemic region of the LV in WT and *Camp* KO mice 3 hours post-reperfusion (n=4 mice per group). (I,J) Quantitative analysis of *Tgf-β* (I) and *Il-10* (J) mRNA in the non-ischemic region of the LV in WT and *Camp* KO mice 3 hours post-reperfusion (n=4 mice per group). Data are shown as mean ± SEM. N.S., no significance; AAR, the area at risk for infarction; NAAR, the non-area at risk for infarction; I/R, ischemia/reperfusion.

Figure 7 Neutrophils might be a main cellular target of cathelicidin in MI/R injury. (A) At 24 hours post-reperfusion, quantitative analysis of infarct size in *Tlr4*^{fl/fl} and *Tlr4*^{MKO} mice injected with vehicle or CRAMP (200 µg/mouse, i.p.) just before MI/R (n=8-10 mice per group. scale bar, 1mm). (B) WT mice were injected i.p. with Clo-Lip (200 µl/mouse) or Con-Lip as a control to deplete cardiac macrophages. After 24 hours, the mice were

administered with vehicle or CRAMP (200 µg/mouse, i.p.) just before MI/R, and then infarct size was measured 24 hours post-reperfusion (n=8-10 mice per group. scale bar, 1mm). (C) Anti-Ly6G (100 µg/mouse) or isotype control antibodies were i.p. injected in WT mice to deplete neutrophils. After 24 hours, the mice were treated with vehicle or CRAMP (200 µg/mouse, i.p.) immediately before MI/R. Infarct size was determined 24 hours post-reperfusion (n=7-12 mice per group. scale bar, 1mm). Data are shown as mean ± SEM. * $P < 0.05$, ** $P < 0.01$ and *** $P < 0.001$. N.S., no significance; LV, the left ventricle; AAR, the area at risk for infarction; IA, the infarct area; I/R, ischemia/reperfusion; Con-Lip, control liposomes; Clo-Lip, clodronate liposomes.

Figure 8 Depletion of cardiac macrophages in mice. WT mice were i.p. injected with Clo-Lip (200 µl/mouse) or Con-Lip as a control to deplete cardiac macrophages. The hearts were collected to confirm the depletion of cardiac macrophages by flow cytometry 24 hours after injection (n=3 mice per group). Data are shown as mean ± SEM. * $P < 0.05$. Con-Lip, control liposomes; Clo-Lip, clodronate liposomes.

Figure 9 Higher TLR4 protein expression in infiltrating neutrophils at ischemia. WT mice were challenged to ischemia for 45 minutes, and then the ischemic area of the LV was collected and subjected to MACS sorting followed by Western blotting. Representative immunoblots showing TLR4 and GAPDH abundance in Ly6G⁺ neutrophils, CD11b⁺Ly6G⁻ myeloid cells, and CD11b⁻Ly6G⁻ non-myeloid cells (left) and semiquantification of band intensities (right) (n=3 independent experiments). Data are shown as mean ± SEM. * $P < 0.05$ and ** $P < 0.01$. AAR, the area at risk for infarction.

Figure 10 Schematic diagram depicting the cathelicidin pathway in the heart in MI/R.
 ① Upon cardiac ischemia, circulating neutrophils are rapidly recruited to the injured myocardium through the injured area, leading to a local release and cleavage of cathelicidin. ② Cleaved cathelicidin stimulates TLR4 signaling and P2X₇R/NLRP3 inflammasome in infiltrating neutrophils, which leads to excessive secretion of IL-1β from neutrophils. ③ Secreted IL-1β results in myocardial inflammatory burst and ultimately tissue post-reperfusion injury. AAR, the area at risk for infarction; NAAR, the non-area at risk for infarction.

Table 1 Primers used for genotyping analysis for *Tlr4*^{fl/fl} and *Tlr4*^{MKO} mice.

Table 2 Echocardiographic data of WT and *Camp* KO mice. Baseline cardiac phenotype of 10-12 week-old *Camp* KO mice and their WT littermates. Data are shown as mean ± SEM.

Highlights

1. Infiltrating neutrophil-derived cathelicidin is increased in response to myocardial ischemia/reperfusion
2. Cathelicidin aggravates myocardial ischemia/reperfusion injury via a TLR4- and P2X₇R/NLRP3 inflammasome-dependent mechanism
3. Cathelicidin promotes IL-1 β secretion from infiltrating neutrophils and enhances myocardial inflammation during myocardial ischemia/reperfusion injury

Journal Pre-proof

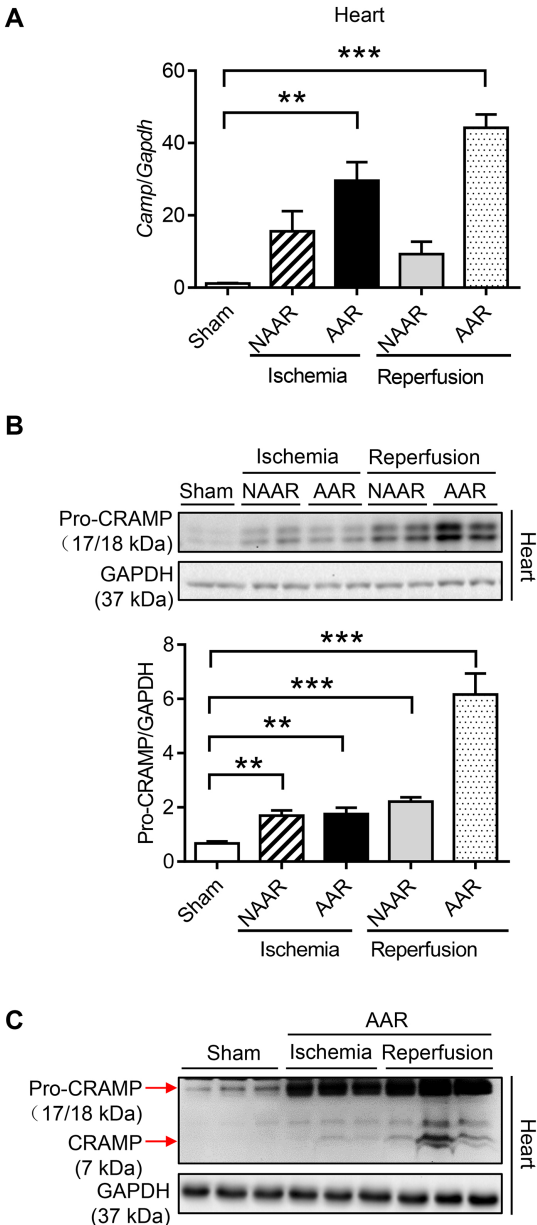


Figure 1

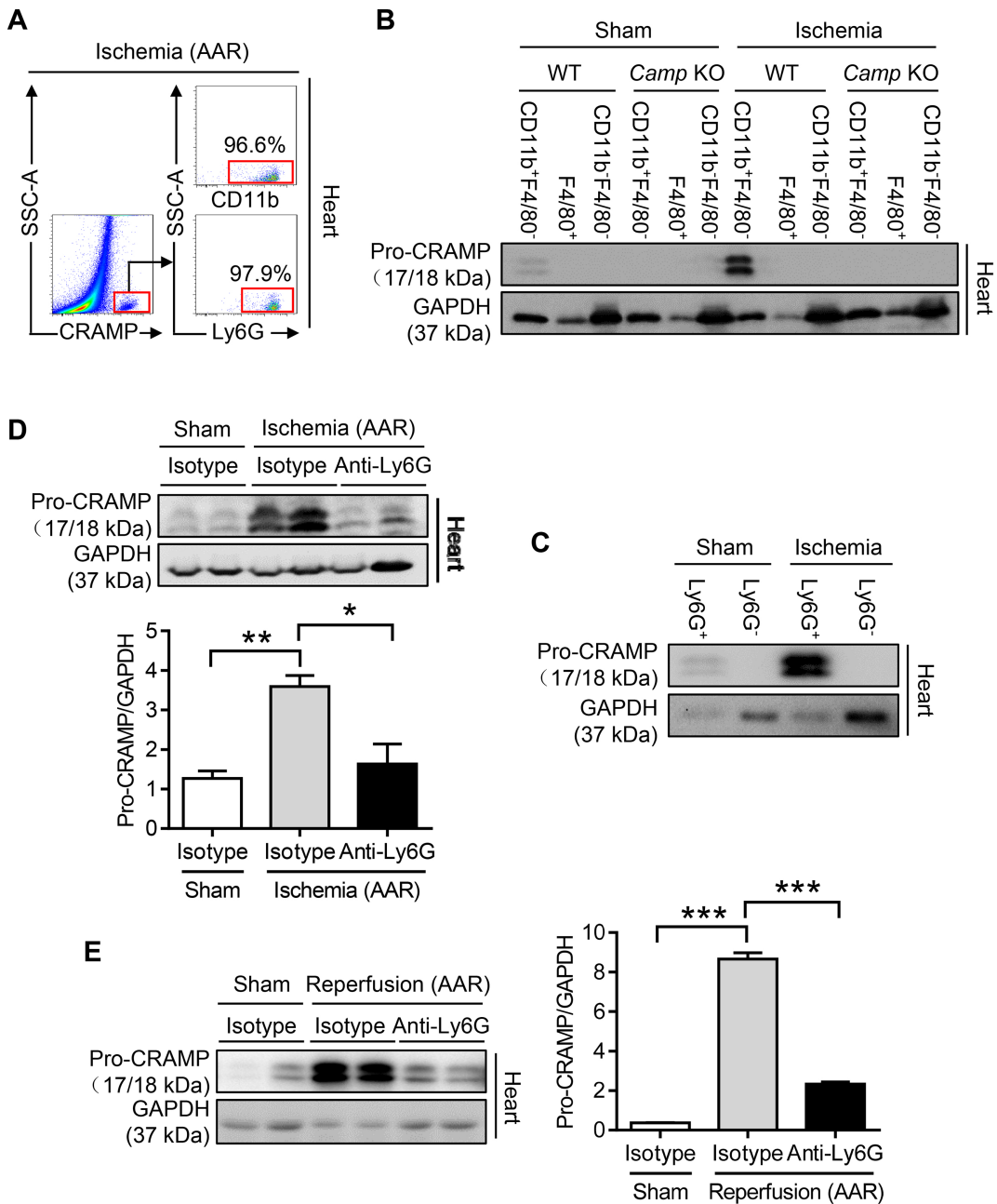


Figure 2

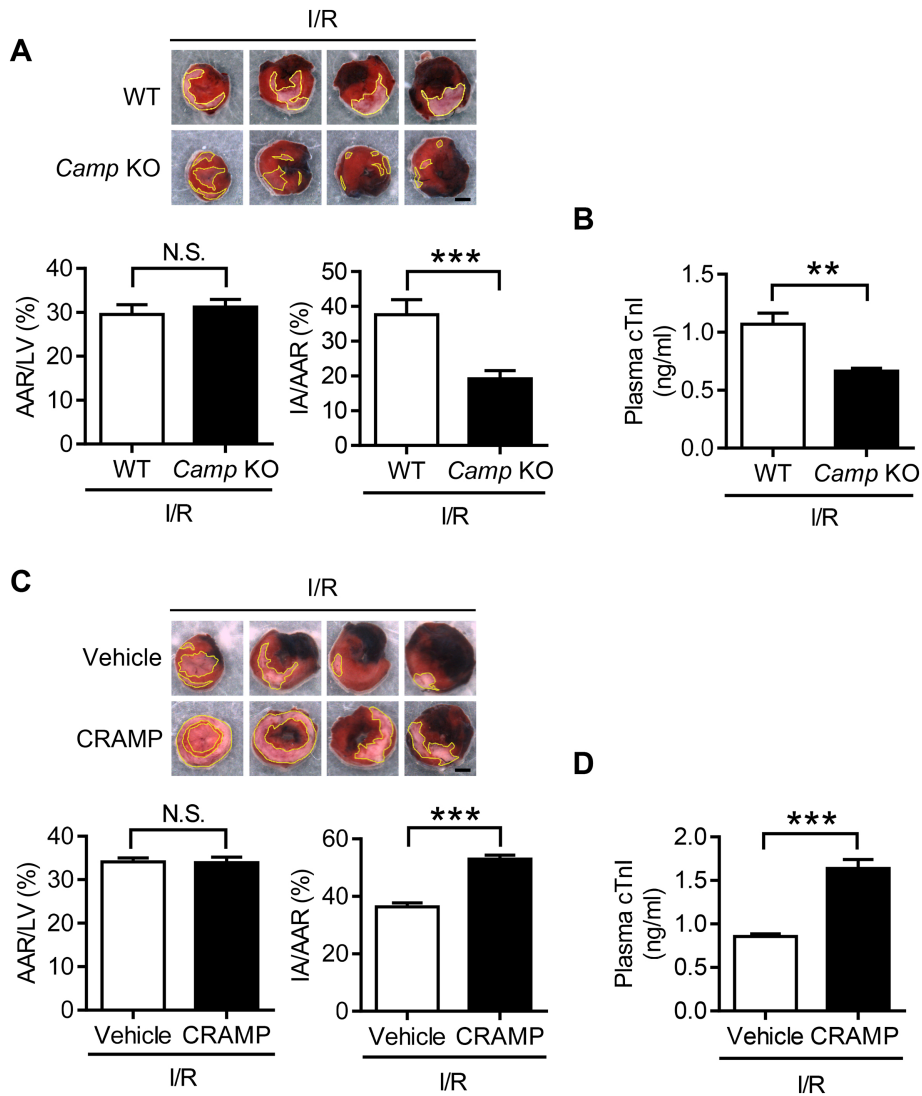


Figure 3

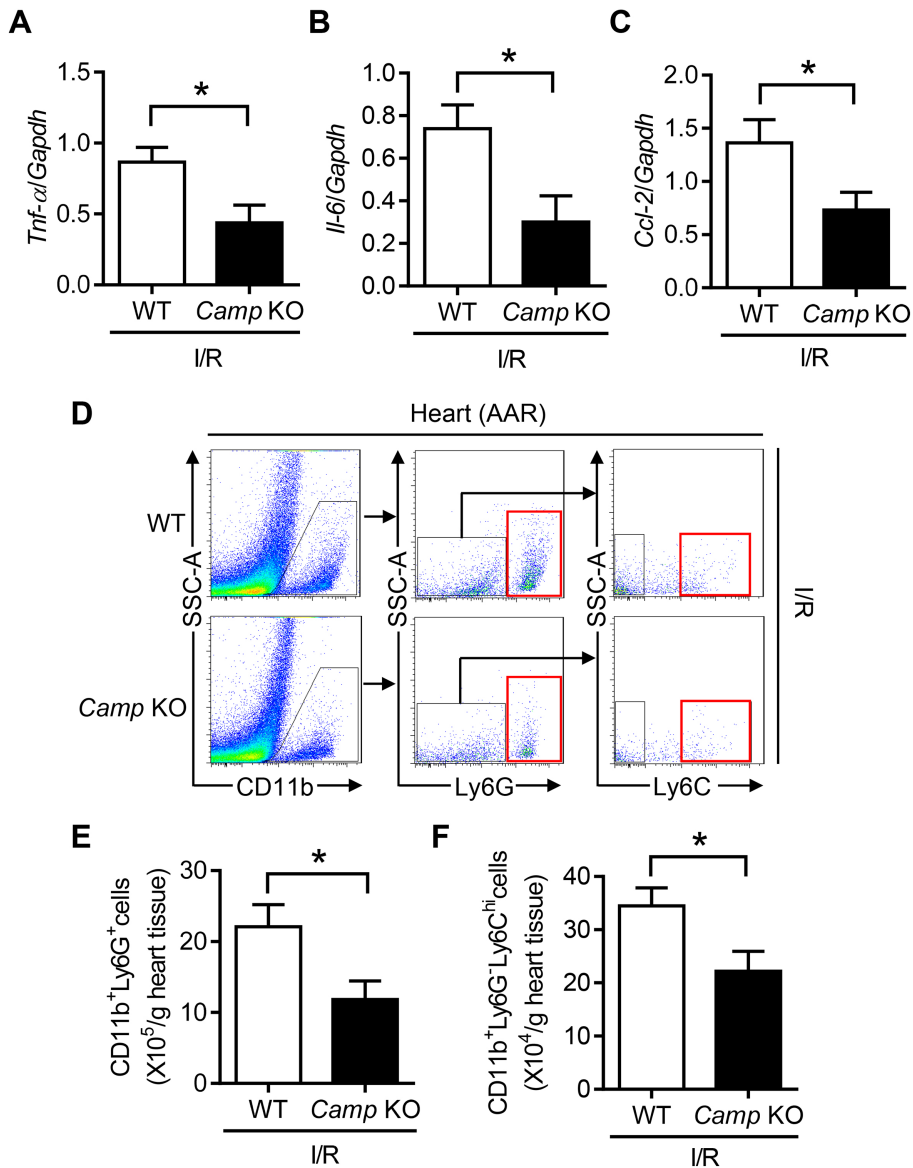


Figure 4

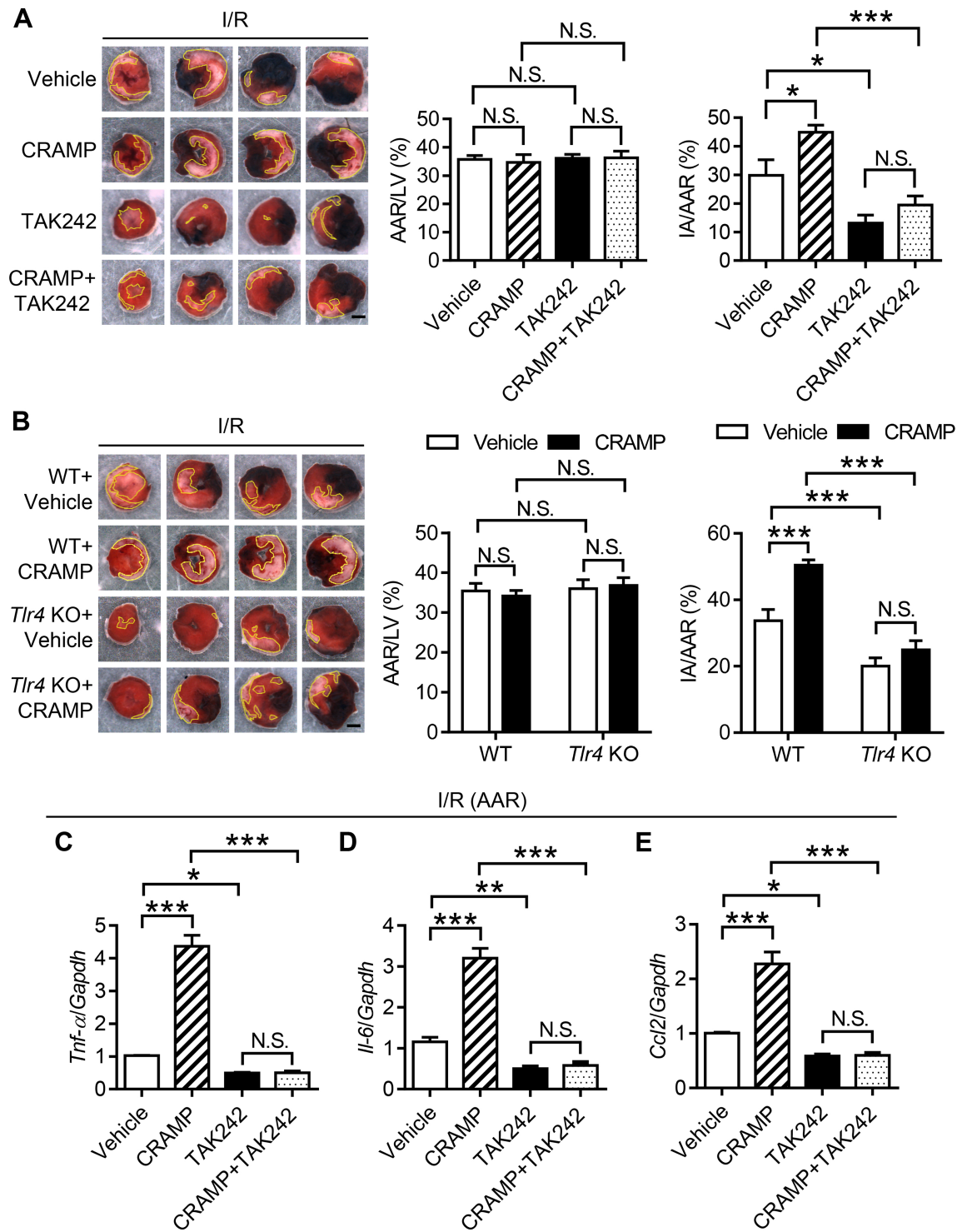


Figure 5

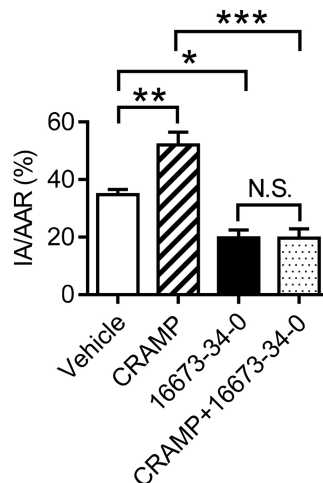
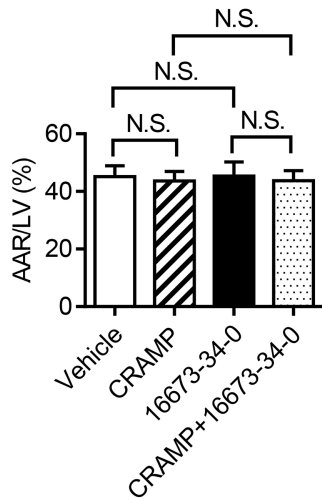
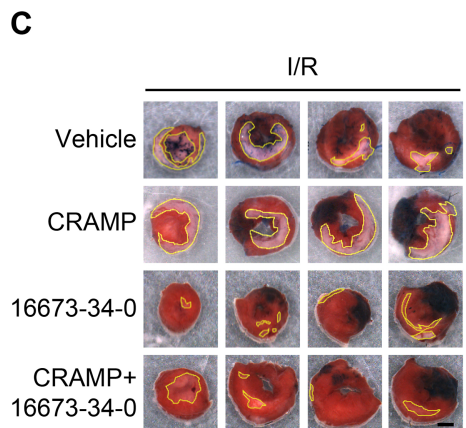
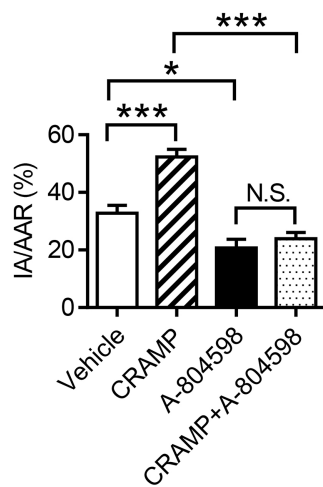
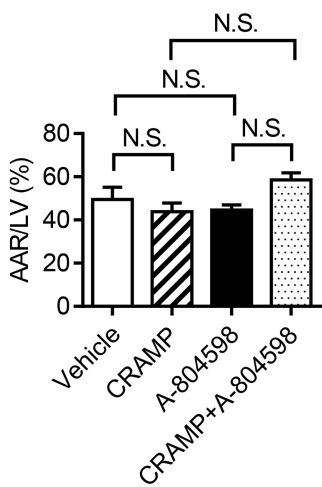
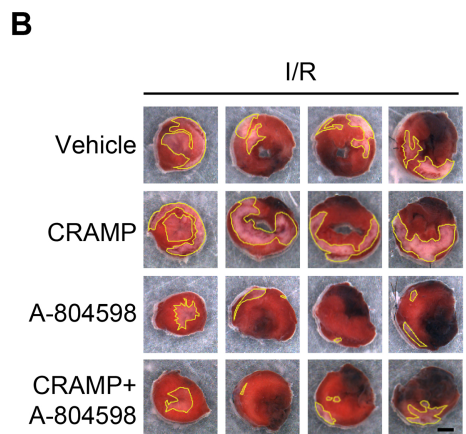
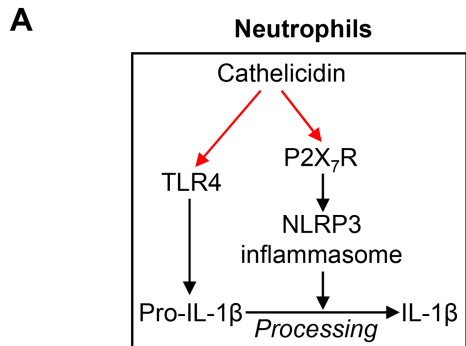
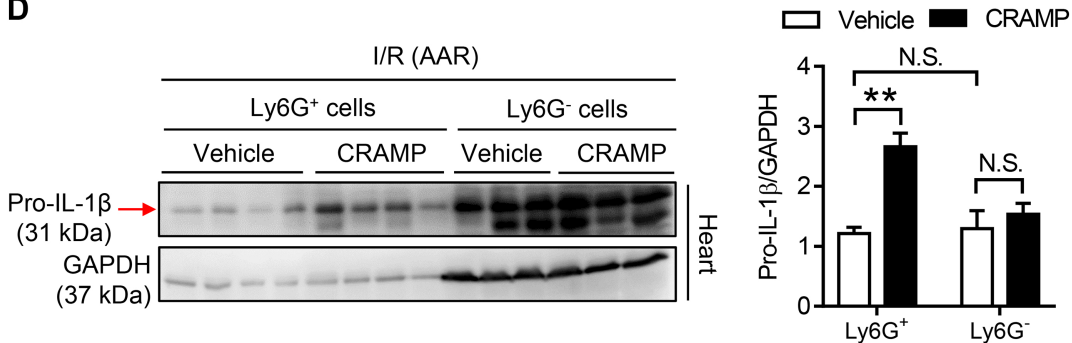


Figure 6A

D

Human neutrophils

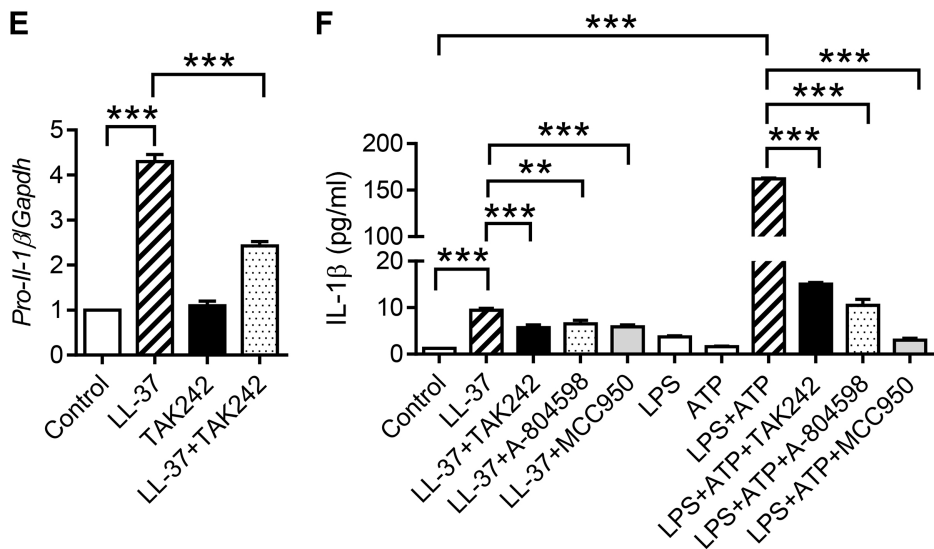


Figure 6B